PROTEIN STRUCTURE REPORT

Crystal structure of yeast YHR049W/FSH1, a member of the serine hydrolase family

SOPHIE QUEVILLON-CHERUEL,[1] NICOLAS LEULLIOT,[1] MARC GRAILLE,[1] NADÈGE HERVOUET,[2] FRANK COSTE,[2] HÉLÈNE BÉNÉDETTI,[2] CHARLES ZELWER,[2] JOEL JANIN,[3] AND HERMAN VAN TILBEURGH[1]

[1]Institut de Biochimie et de Biophysique Moléculaire et Cellulaire (CNRS-UMR 8619), Université Paris-Sud, 91405 Orsay, France
[2]Centre de Biophysique Moléculaire (CNRS-UPR4301), 45071 Orleans Cedex 02, France
[3]Laboratoire d'Enzymologie et Biochimie Structurales (CNRS-UPR 9063), 91198 Gif sur Yvette, France

(RECEIVED February 15, 2005; FINAL REVISION February 15, 2005; ACCEPTED February 18, 2005)

Abstract

Yhr049w/FSH1 was recently identified in a combined computational and experimental proteomics analysis for the detection of active serine hydrolases in yeast. This analysis suggested that FSH1 might be a serine-type hydrolase belonging to the broad functional αβ-hydrolase superfamily. In order to get insight into the molecular function of this gene, it was targeted in our yeast structural genomics project. The crystal structure of the protein confirms that it contains a Ser/His/Asp catalytic triad that is part of a minimal α/β-hydrolase fold. The architecture of the putative active site and analogies with other protein structures suggest that FSH1 may be an esterase. This finding was further strengthened by the unexpected presence of a compound covalently bound to the catalytic serine in the active site. Apparently, the enzyme was trapped with a reactive compound during the purification process.

Keywords: esterase; lipase; Yhr049w/FSH1; serine hydrolase; OVCA2; Ymr222c/FSH2; Yor280c/FSH3

Structural proteomics aims at large-scale determination of protein structures. One of the goals of structural proteomics projects is to construct a dictionary of folds against which every sequence from the protein universe could be modeled with some degree of confidence. In many of the large-scale projects, proteins for which no structural homolog is available at the 30% sequence identity level are targeted. A structural targets list of many of these projects is available from http://targetdb.pdb.org/. Our Yeast Structural Genomics project (http://genomics.eu.org/spip/index.php) targeted 300 soluble proteins of unknown structure. A global overview of this project was recently published (Quevillon-Cheruel et al. 2004).

Structural genomics targets are frequently of unknown or only poorly known biochemical function. Because protein structure is much better conserved than sequence, comparison of these new structures with those of known function may provide insight into biochemical function. This opened up a new area of research in the field of structure–function relationships (Fetrow et al. 1999; Orengo et al. 1999; Yakunin et al. 2004). Three main strategies are currently applied for the deduction of function from structure: The new structure reveals (1) analogies with a protein of known function that could not be predicted from sequence alone (Liger et al. 2004), (2) unexpected bound molecules present in the crystal that were co-purified from the bacterial broth (Zarembinski et al. 1998; Zhou et al. 2005), and (3) some functional features that were not predicted from sequence, for instance, the presence of a catalytic triad (de La Sierra-Gallay et al. 2004; Graille et al. 2004). The latter method frequently makes use of databases of structural templates derived from active sites of multiple classes of enzymes (Porter et al. 2004). This is based on the strong conservation of spatial positions of catalytic residues within a functional class of enzymes even if substrate specificities and protein folds vary greatly within the same functional class.

Reprint requests to: Herman van Tilbeurgh, Institut de Biochimie et de Biophysique Moléculaire et Cellulaire (CNRS-UMR 8619), Université Paris-Sud, Bâtiment 430, 91405 Orsay, France; e-mail: Herman.Van-Tilbeurgh@ibbmc.u-psud.fr; fax: +33-1-69-85-37-15.

Article published online ahead of print. Article and publication date are at http://www.proteinscience.org/cgi/doi/10.1110/ps.051415905.

In order to help with the functional assignment of the proteome, approaches aimed at functional analysis are being developed. One such approach proposed the combination of chemical and computational proteomics to introduce new protein members of the yeast proteome into documented functional classes. A recent systematic study endeavored to identify all the serine hydrolase enzymes from yeast (Baxter et al. 2004). The first approach consisted of computational analysis using templates derived from serine hydrolase active sites. The second experimental approach used specialized chemical probes. These probes contain a chemical group able to react with a wide variety of enzymes (broad specificity), which is attached to a chemical label that allowed the retrieval of reactive proteins from a complex mixture. An overlapping set of 15 proteins were identified by both methods, eight of which were of unknown function. Three of the eight potential serine hydrolase/carboxylesterases (FSH1 or YHR049wp, FSH2 or YMR222cp, and FSH3 or YOR280cp) are members of a new eukaryotic serine hydrolase family (FSH: family of serine hydrolases) that encompasses OVCA2, a potential human tumor suppressor (Schultz et al. 1996; Huang et al. 2000). The yeast FSH proteins also have sequence analogs in other eukaryotic organisms, none of which have annotated functions.

The *Yhr049w/FSH1* gene encodes for a 27-kDa protein with unknown function, which was selected as a target of our yeast structural genomics project (Quevillon-Cheruel et al. 2003, 2004). Here we present its crystal structure at 1.7 Å resolution, confirming that FSH1 belongs to the αβ-hydrolase superfamily. Moreover, the crystal structure reveals the presence of a covalently bound compound attached to the active site serine, suggesting an implication of FSH1 in the hydrolysis of hydrophobic phosphonate ester compounds.

Results and Discussion

Overall structure

The structure was determined using a Se-methionine substituted protein by single anomalous dispersion to a resolution of 1.7 Å. Most of the peptide chain had well-defined electron density except for a few N- and C-terminal residues (see Materials and Methods). FSH1 has one or two copies in the asymmetric unit in the Se-Met and native crystals, respectively.

At the end of the refinement, the electron density revealed the presence of a point mutation: Residue Phe109 in the wild-type sequence was unintentionally mutated into leucine during the gene amplification process. Apparently this mutation was well tolerated in the structure, although Phe109 is an absolutely conserved residue in the FSH1 family (see below).

As observed in Figure 1A, FSH1 has an overall αβ class fold with a six-stranded central parallel β-sheet sandwiched between major helices. The order of the strands is β2β1β3β4β7β8. A full helix (α2) and two more short helical turns connecting β2 and α3 form a cap-like extension. A small β-sheet (β5β6) is located at the opposite site of this cap. These extensions define a groove that forms the active site of FSH1. The structure belongs to the well-documented αβ-hydrolase superfamily containing hydrolases with various enzymatic activities (Heikinheimo et al. 1999; Nardini and Dijkstra 1999). The canonical α/β-hydrolase fold is characterized by an eight-stranded mostly parallel αβ structure with strand β2 anti-parallel to the others. Yhr049w/FSH1 misses the first two strands, β1 and β2, from the canonical fold, a characteristic shared by many other hydrolases, such as bacterial lipase (van Pouderoyen et al. 2001), cutinase (Martinez et al. 1992), human brain platelet activating factor (Ho et al. 1999), and *Streptomyces scabies* esterase (Wei et al. 1995).

A nucleophile/histidine/acid triad forms the basic catalytic machinery of all αβ-hydrolases, but the nature of the nucleophilic and acidic residues varies between different families: cysteine, serine (majority), or even aspartate (e.g., haloalkane dehalogenase) are observed as nucleophiles and aspartate/glutamate as acids. FSH1 clearly has a well-confined pocket that harbors such a triad of residues, highly likely to represent the catalytic site of the protein. The triad consists of a putative nucleophile Ser110, situated in an expected tight turn between strand β3 and helix α4, completed by His218 (from the loop after strand β8) and Asp183 (after strand β7). These positions correspond to those observed for the catalytic triad residues in the canonical αβ-hydrolase fold (Heikinheimo et al. 1999). The nucleophile in αβ-hydrolases is invariably at the corner of a tight turn (the "nucleophile elbow") with unfavorable Ramachandran angles (Ollis and Goldman 1992; Nardini and Dijkstra 1999). These properties are observed for the putative FSH1 nucleophile Ser110. Two main-chain nitrogens belonging to residues Phe14 and Gln111 are in a correct position relative to the Ser110 Oγ atom to form an oxyanion hole that contributes to the catalytic machinery and is involved in electrophilic stabilization of the developing negative charge during catalysis (see below).

The residues of the catalytic triad are situated in a confined groove at the C terminal of the central sheet. The floor of this groove is formed by residues 141–144 at the end of strand β4. The walls are formed by residues 74–81 (long loop at the end of strand β2), Phe14 after strand β1, and Val186 after strand β5.

Comparison with other α/β-hydrolases

Structure alignment using the MSD server (http://www.ebi.ac.uk/msd-srv/ssm/) revealed that FSH1 is most similar

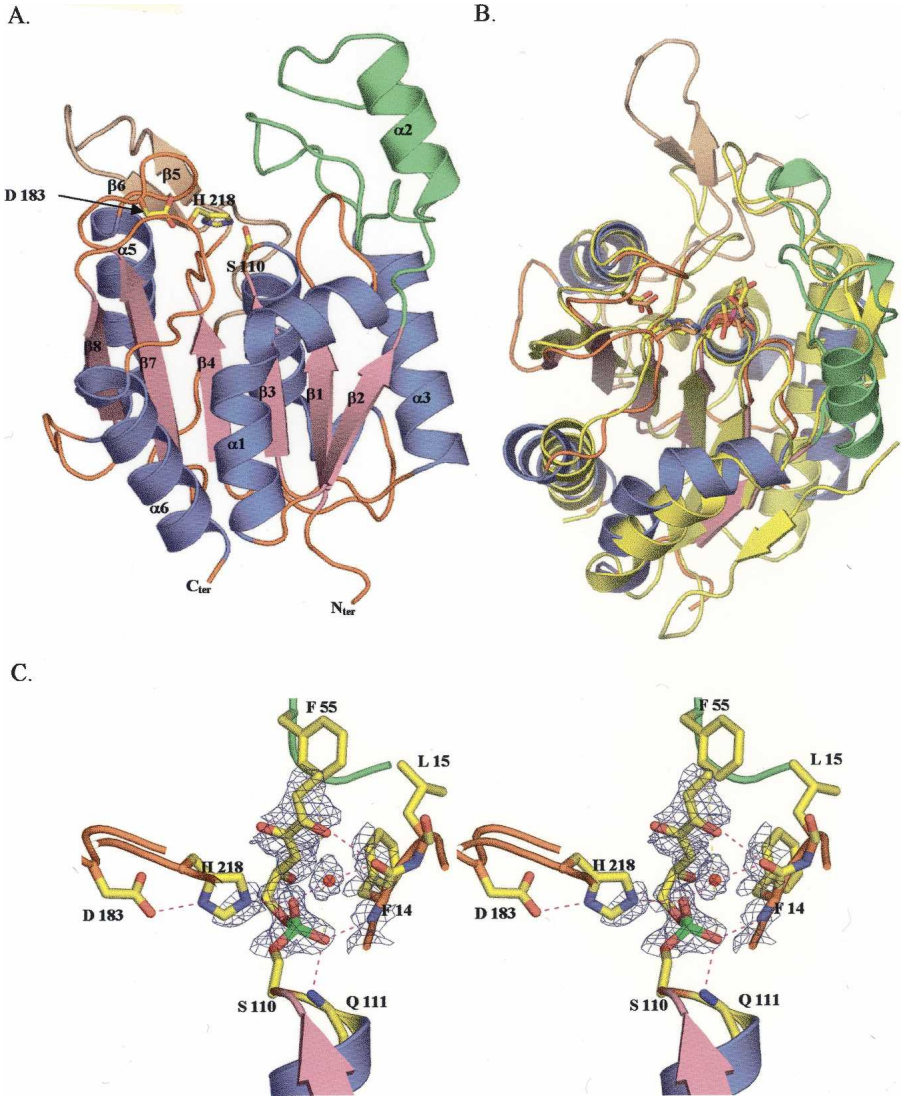

Figure 1. The structure of FSH1. (*A*) Ribbon representation of FSH1. Helices, strands, and loops are colored blue, pink, and orange, respectively. Insertions relative to the canonical α/β-hydrolase fold are colored green (cap) and beige (β-sheet β5–β6). The catalytic triad residues (Ser110, His218, and Asp183) are shown as sticks. (*B*) Superimposition of the *P. fluorescens* carboxylesterase (yellow, PDB code 1AUR) structure on the *S. cerevisiae* FSH1 protein (same color code as Fig. 1A). Residues of the catalytic triads as well as the molecules covalently bound to FSH1 and carboxylesterase catalytic Ser are shown as sticks. (*C*) Stereo view of the 2Fo-Fc electron density map contoured at 1σ (blue). The molecule covalently bound to Ser110 has been omitted for calculation of this map. For clarity, the map is only drawn around the Ser110 residue. This density was modeled by a phospho-ester compound (P atom in green). Dotted lines depict potential hydrogen of the bound compound.

to carboxylesterase from *Pseudomonas fluorescens* (PDB code 1aur, Z score 8.2, rmsd 1.98 Å for 164 Cα positions), protein TT1162 from *Thermus thermophilus* (PDB code 1ufo, Z score 7.9, rmsd 1.95 Å for 155 Cα positions), human acyl protein thioesterase (PDB code 1fj2, Z score 7.9, rmsd 1.98 Å for 171 Cα positions), and 2 hydroxy-6-oxo-6-phenylhexa-2,4-dienoatehydrolase from *Rhodococcus sp.* (PDB code 1c4x, Z score 7.7, rmsd 2.05 Å for 154 Cα positions). Sequence identity between FSH1 and these structural analogs is around 16%. Similar structural analogies were further detected with other esterases, lactamases, and peroxidases.

Carboxylesterase and acyl protein thioesterase both have an extra strand compared with FSH1 and TT1162 has two, but their core is otherwise extremely well conserved (Fig. 1B). The loop extensions around the active site groove in carboxylesterase and acyl protein thioesterase are shorter than those of FSH1, while those in TT1162 are comparable. Therefore all of these enzymes share very similar molecular architectures.

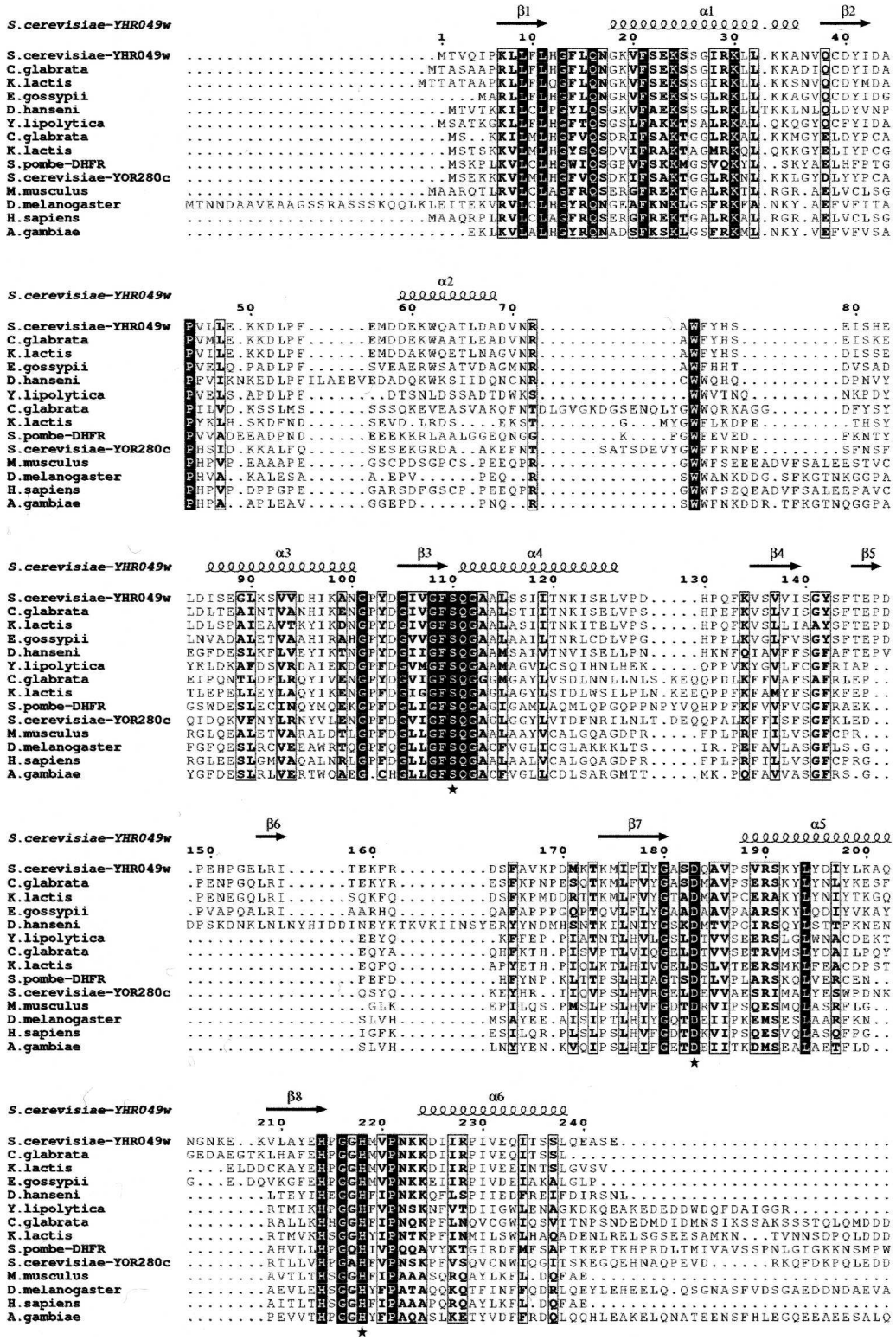

Figure 2. Structure-based sequence alignment of the FSH1 protein family. The alignment was obtained using CLUSTALW at http://www.ebi.ac.uk/clustalw/ (Thompson et al. 1994). Residue numbering refers to the sequence of YHR049wp from *S. cerevisiae*. Secondary structure elements were obtained for the structure of YHR049wp using the ESPript server (Gouet et al. 1999). Strictly conserved residues are in white on a black background. Partially conserved amino acids are boxed. Residues forming the catalytic triad are indicated by black stars *below* the alignment.

Residual electron density at the active site

After refinement of the structure, strong residual electron density remained present in the putative active site pocket. Continuous electron density extended from Ser110 Oγ toward the exit of the pocket, suggesting that some compound is covalently attached. Since no reactive compounds such as protease inhibitors were added on purpose during the purification/crystallization process, we presume a molecule present in the cellular broth reacted with the FSH1 active serine to yield a stable adduct. This residual electron density had a strong maximum (6σ level) next to the Ser110 Oγ position. The strength of the peak and its distance from the Ser Oγ position is compatible with either a sulfur or phosphorous atom. The density around this position reveals a tetrahedral configuration. In the recently determined structure of BIOH, a close FSH1 structural analog involved in biotin synthesis in *Escherichia coli*, the investigators observed unintentional covalent modification of the active site serine by PMSF, added during the purification process (Sanishvili et al. 2003).

Overwhelming evidence has been accumulated that catalytic triad esterases and proteases proceed through formation of a covalent tetrahedral intermediate. The lifetime of this intermediate is usually extremely short and can only be "visualized" in the case of activated compounds and/or active site mutants (Egloff et al. 1995). The reason why we observe a covalent adduct in our FSH1 crystal structure is not clear. Although the present Phe109Leu mutation is situated next to the active site serine and hence may influence the reaction kinetics and/or substrate specificity, it is not expected that this type of mutation would lead to a stable covalent intermediate. The strength and form of the residual electron density cloud clearly indicates that either a tetrahedral phosphate or sulfate atom is attached to Ser110 Oγ (Fig. 1C). A well-defined oxygen is pointing toward the two main-chain nitrogen atoms of the oxyanion hole (at 2.72 Å and 2.64 Å of N-Phe14 and N-Gln111, respectively). The second oxygen forms a hydrogen bond to Nε2 from His218. The fourth position of the bound compound has an elongated shape, suggesting that it represents an alkyl moiety. A part of the alkyl region of a phospholipid group was modeled into the density. The alkyl group is lying in a hydrophobic groove consisting of Phe14 and Leu15 from the β1α1 connection and Leu53, Pro54, Phe55, and Met57 from the cap extension. Therefore the bound compound mimics the first tetrahedral intermediate in the cleavage reaction of ester compounds.

In order to gain insight into the possible substrate preference of FSH1, we superposed our structure with lipases and esterases containing covalently bound inhibitors in the active site. Figure 1B shows the superimposition of the active site of *P. fluorescens* carboxylesterase (CE) with its catalytic Ser Oγ bound to a phenylmethyl-sulfonyl moiety (Kim et al. 1997) and our FSH1 bound compound. As can be seen, the CE-PMSF superposes well with our putative phosphonyl compound. The FSH1 catalytic Nε2 of His218 is at 3.8 Å of the putative phosphorous position and hydrogen bonding to the Ser110 Oγ atom. The native structure (with covalent adduct) and the Se-methionine (apo)structure are identical. This suggests that the FSH1 oxyanion hole is preformed and not induced upon substrate binding as is the case of many lipases (e.g., Rhizomucor lipase [Brzozowski et al. 1991]).

Molecular function of FSH1

FSH1 was identified from a large-scale study using two complementary approaches: computational prediction of serine active site hydrolases and exploitation of their chemical reactivity in complex mixtures (Baxter et al. 2004). FSH1 is member of a new eukaryotic serine hydrolase family. This family includes two other yeast analogs: FSH2 (Ymr222c) and FSH3 (Yor280c) as well as OVCA2, a potential tumor suppressor (Huang et al. 2000), and DYR-_SCHPO, annotated as a dihydrofolate reductase from *Schizzosaccharomyces pombe* (Fig. 2). The yeast FSH sequences have only very low pairwise sequence identity (21%). The activity-based probes were biotinylated fluorophosphonates. These very reactive compounds are believed to form adducts with a large fraction of existing serine hydrolases. Our present structure confirms that FSH1 belongs to the α/β-hydrolase fold family and that it has a typical catalytic Asp/His/Ser triad. The compound that is covalently bound to the active serine could not be chemically identified, but it probably represents a partial degradation product of a phospholipid moiety. It is not clear whether the observed adduct is related to the biochemical activity of FSH1 in vivo, especially since αβ-hydrolases catalyze a wide variety of reactions. The hydrophobic nature of the FSH1 active site pocket suggests that it may be involved in the hydrolysis of lipidic ester compounds. The residual electron density connected to Ser110 was not observed from protein purified from minimal medium cultured cells (data not shown).

The annotation of the *S. pombe* ortholog as a DHFR is due to gene fusion between a FSH1 ortholog and DHFR for this organism. It is not clear whether this could represent a functional link between these two activities (this coupling seems to be a unique event since it was not observed today in other genomics sequences). There is no information on the cellular function of FSH1.

Materials and methods

Cloning, expression, and purification

ORF *YHR049w* was amplified by PCR using the genomic DNA of *S. cerevisiae* strain S288C as a template. An additional sequence

Table 1. *Data collection, phasing, and refinement statistics*

Data collection	SAD (peak)	Native
Wavelength	0.9795	0.9750
Resolution (Å)	40–2.35 (2.48–2.35)	20–1.7 (1.78–1.7)
Space group	$P2_12_12_1$	P1
Unit cell parameters (Å,°)	a = 45.8; b = 68.7; c = 80.5	a = 46; b = 53.3; c = 64.3; $\alpha = 102.85$; $\beta = 90$; $\gamma = 112.5$
Total number of reflections	75,623	100,787
Total number of unique reflections	10,941	57,009
R_{sym} (%)[a]	0.10 (0.56)	0.047 (0.165)
Completeness (%)	98.9 (98.9)	94.8 (91.2)
I/σ (I)	6.9 (1.3)	14.6 (3.7)
Redundancy	6.9	1.8
Phasing		
Resolution (Å)	40–2.35	
Figure of merit	0.28	
Refinement		
Resolution (Å)		20–1.7
R/R_{free} (%)[b]		16.5/20.2
R.m.s.d. bonds (Å)		0.011
R.m.s.d. angles (°)		1.283
Ramachandran plot (%)		
Most favored		92
Allowed		7.4

Values in parentheses are for highest resolution shell. (SAD) Single wavelength anomalous dispersion.
[a] $R_{sym} = \sum_h\sum_i|I_{hi} - \langle I_h\rangle|/\sum_h\sum_i I_{hi}$, were I_{hi} is the i^{th} observation of the reflection h, while $\langle I_h\rangle$ is the mean intensity of reflection h.
[b] $R_{factor} = \sum ||F_o| - k|F_c||/\sum|F_o|$. R_{free} was calculated with a small fraction (5%) of randomly selected reflections.

coding for a six-histidine tag was introduced at the 3′ end of the gene during amplification. The PCR product was then cloned between the NcoI and the NotI restriction sites of pET28 vector (Stratagene). Expression was done at 37°C using the transformed *E. coli* Rosetta(DE3)pLysS strain and 2xYT medium (BIO101 Inc.) supplemented with kanamycin at 50 μg/mL. When the cell culture reached an $OD_{600\ nm}$ of 1, protein expression was induced with 0.3 mM IPTG (Sigma) and the cells were grown for a further 4 h. Cells were harvested by centrifugation; resuspended in 40 mL of 20 mM Tris-HCl at pH 7.5, 200 mM NaCl, and 5 mM β-mercaptoethanol; and stored overnight at −20°C. Cell lysis was completed by sonication. The His-tagged protein was purified on a Ni-NTA column (Qiagen Inc.), eluted with imidazole, and loaded onto a SuperdexTM200 column (Amersham Pharmacia Biotech) equilibrated against 20 mM Tris-HCl at pH 7.5, 200 mM NaCl, and 10 mM β-mercaptoethanol. Se-Met labeled protein was prepared as described and purified as the native protein (Quevillon-Cheruel et al. 2004). The homogeneity of the proteins was checked by SDS-PAGE, and the labeling degree by mass spectrometry.

Crystallization and resolution of the structure

Native and Se-Met labeled protein samples were stored in 20 mM Tris-HCl at pH 7.5, 200 mM NaCl, and 10 mM β-mercaptoethanol. Crystals of both the native and Se-Met labeled protein were grown from a 1:1-μL mixture of protein (15 mg/mL) with 27% PEG4000, 0.1 M MES at pH 5.6, and 0.5 M lithium acetate (Se-Met) and 25% PEG4000 and 0.1 M MES at pH 6.5 (native). For the Se-Met labeled protein, crystals with a maximal size of 100–200 μ appeared within 1 d. For the native protein, highest diffraction was obtained from a triclinic crystal (other data not shown). For data collection, the crystals were frozen in liquid nitrogen after successive transfer in cryoprotectant buffer containing the reservoir solution plus 10%, 20%, and 30% ethylene glycol. Crystals of the native and Se-Met labeled proteins diffracted to 1.7 Å and 2.35 Å, respectively (beamline BM14 at the European Synchrotron Radiation Facility, Grenoble, France).

The structure was determined using single wavelength anomalous dispersion (SAD) X-ray diffraction data, collected from the Se-Met derivative crystal. Data were processed using the program MOSFLM (Kabsch 1993). The space group was $P2_12_12_1$ with one molecule per asymmetric unit. Four selenium atom sites out of five were found for each monomer with the program SHELXD in the 20–2.35 Å resolution range (Schneider and Sheldrick 2002). The Sharp suite was used for phasing and upon inspection of the residual maps, a fifth selenium site corresponding to an alternate conformation for Met171 was identified and used for phasing (Bricogne et al. 2003). After solvent flattening and phase extension to 2.35 Å resolution with the program RESOLVE (Terwilliger 2003), the quality of the electron density map allowed the manual construction of most of the secondary structure elements with the TURBO molecular modeling program (Roussel and Cambillau 1991).

This preliminary model, built using electron density maps calculated with experimental phases, was then used as search model for molecular replacement trials with data collected from a triclinic crystal to 1.7 Å resolution. Two molecules were positioned in the asymmetric unit with the program MOLREP (Vagin and Isupov 2001). This model was completed using iterative cycles of model building with TURBO and refinement with the REFMAC program (Murshudov et al. 1997). The final model contains residues 3–239 from monomer A, residues 4–241 from monomer B, and 936 water molecules. Except for Ser110 (from both monomers), all residues

fall within the allowed regions of the Ramachandran plot as defined by the program PROCHECK (Laskowski et al. 1993). Analysis of the residual electron density maps revealed that Ser110 is covalently bound to a molecule that has been modeled as a phospholipid tail. Data collection and refinement statistics of the structure are summarized in Table 1. The atomic coordinates and structure factors for the protein structure have been deposited into the Brookhaven Protein Data Bank under the accession number 1YCD.

Acknowledgments

M.G. benefits from a grant of the Association pour la Recherche sur le Cancer (ARC).

References

Baxter, S.M., Rosenblum, J.S., Knutson, S., Nelson, M.R., Montimurro, J.S., Di Gennaro, J.A., Speir, J.A., Burbaum, J.J., and Fetrow, J.S. 2004. Synergistic computational and experimental proteomics approaches for more accurate detection of active serine hydrolases in yeast. *Mol. Cell. Proteomics* **3:** 209–225.

Bricogne, G., Vonrhein, C., Flensburg, C., Schiltz, M., and Paciorek, W. 2003. Generation, representation and flow of phase information in structure determination: Recent developments in and around SHARP 2.0. *Acta Crystallogr. D Biol. Crystallogr.* **59:** 2023–2030.

Brzozowski, A.M., Derewenda, U., Derewenda, Z.S., Dodson, G.G., Lawson, D.M., Turkenburg, J.P., Bjorkling, F., Huge-Jensen, B., Patkar, S.A., and Thim, L. 1991. A model for interfacial activation in lipases from the structure of a fungal lipase-inhibitor complex. *Nature* **351:** 491–494.

de La Sierra-Gallay, I.L., Collinet, B., Graille, M., Quevillon-Cheruel, S., Liger, D., Minard, P., Blondeau, K., Henckes, G., Aufrere, R., Leulliot, N., et al. 2004. Crystal structure of the YGR205w protein from *Saccharomyces cerevisiae*: Close structural resemblance to *E. coli* pantothenate kinase. *Proteins* **54:** 776–783.

Egloff, M.P., Marguet, F., Buono, G., Verger, R., Cambillau, C., and van Tilbeurgh, H. 1995. The 2.46 Å resolution structure of the pancreatic lipase-colipase complex inhibited by a C11 alkyl phosphonate. *Biochemistry* **34:** 2751–2762.

Fetrow, J.S., Siew, N., and Skolnick, J. 1999. Structure-based functional motif identifies a potential disulfide oxidoreductase active site in the serine/threonine protein phosphatase-1 subfamily. *FASEB J.* **13:** 1866–1874.

Gouet, P., Courcelle, E., Stuart, D.I., and Metoz, F. 1999. ESPript: Analysis of multiple sequence alignments in PostScript. *Bioinformatics* **15:** 305–308.

Graille, M., Quevillon-Cheruel, S., Leulliot, N., Zhou, C.Z., de la Sierra Gallay, I.L., Jacquamet, L., Ferrer, J.L., Liger, D., Poupon, A., Janin, J., et al. 2004. Crystal structure of the YDR533c *S. cerevisiae* protein, a class II member of the Hsp31 family. *Structure (Camb.)* **12:** 839–847.

Heikinheimo, P., Goldman, A., Jeffries, C., and Ollis, D.L. 1999. Of barn owls and bankers: A lush variety of α/β hydrolases. *Structure Fold. Des.* **7:** R141–R146.

Ho, Y.S., Sheffield, P.J., Masuyama, J., Arai, H., Li, J., Aoki, J., Inoue, K., Derewenda, U., and Derewenda, Z.S. 1999. Probing the substrate specificity of the intracellular brain platelet-activating factor acetylhydrolase. *Protein Eng.* **12:** 693–700.

Huang, J., Hu, N., Goldstein, A.M., Emmert-Buck, M.R., Tang, Z.Z., Roth, M.J., Wang, Q.H., Dawsey, S.M., Han, X.Y., Ding, T., et al. 2000. High frequency allelic loss on chromosome 17p13.3-p11.1 in esophageal squamous cell carcinomas from a high incidence area in northern China. *Carcinogenesis* **21:** 2019–2026.

Kabsch, W. 1993. Automatic processing of rotation diffraction data from crystals of initially unknown symmetry and cell constants. *J. Appl. Crystallogr.* **26:** 795–800.

Kim, K.K., Song, H.K., Shin, D.H., Hwang, K.Y., Choe, S., Yoo, O.J., and Suh, S.W. 1997. Crystal structure of carboxylesterase from *Pseudomonas fluorescens*, an α/β hydrolase with broad substrate specificity. *Structure* **5:** 1571–1584.

Laskowski, R.A., MacArthur, M.W., Moss, D.S., and Thornton, J.M. 1993. PROCHECK: A program to check stereochemical quality of protein structures. *J. Appl. Crystallogr.* **26:** 283–291.

Liger, D., Graille, M., Zhou, C.Z., Leulliot, N., Quevillon-Cheruel, S., Blondeau, K., Janin, J., and van Tilbeurgh, H. 2004. Crystal structure and functional characterization of yeast YLR011wp, an enzyme with NAD(P)H-FMN and ferric iron reductase activities. *J. Biol. Chem.* **279:** 34890–34897.

Martinez, C., De Geus, P., Lauwereys, M., Matthyssens, G., and Cambillau, C. 1992. *Fusarium solani* cutinase is a lipolytic enzyme with a catalytic serine accessible to solvent. *Nature* **356:** 615–618.

Murshudov, G., Vagin, A., and Dodson, E. 1997. Refinement of macromolecular structures by the maximum-likelihood method. *Acta Crystallogr. D Biol. Crystallogr.* **53:** 240–255.

Nardini, M. and Dijkstra, B.W. 1999. α/β Hydrolase fold enzymes: The family keeps growing. *Curr. Opin. Struct. Biol.* **9:** 732–737.

Ollis, D.L. and Goldman, A. 1992. The α/β hydrolase fold. *Protein Eng.* **5:** 197–211.

Orengo, C.A., Todd, A.E., and Thornton, J.M. 1999. From protein structure to function. *Curr. Opin. Struct. Biol.* **9:** 374–382.

Porter, C.T., Bartlett, G.J., and Thornton, J.M. 2004. The Catalytic Site Atlas: A resource of catalytic sites and residues identified in enzymes using structural data. *Nucleic Acids Res.* **32:** D129–D133.

Quevillon-Cheruel, S., Collinet, B., Zhou, C.Z., Minard, P., Blondeau, K., Henkes, G., Aufrere, R., Coutant, J., Guittet, E., Lewit-Bentley, A., et al. 2003. A structural genomics initiative on yeast proteins. *J. Synchrotron. Radiat.* **10:** 4–8.

Quevillon-Cheruel, S., Liger, D., Leulliot, N., Graille, M., Poupon, A., De la Sierra-Gallay, I.L., Zhou, C.Z., Collinet, B., Janin, J., and van Tilbeurgh, H. 2004. The Paris-Sud yeast structural genomics pilot-project: From structure to function. *Biochimie* **86:** 617–623.

Roussel, A. and Cambillau, C. 1991. *TURBO-FRODO, Silicon Graphics Applications Directory*. Silicon Graphics, Mountain View, CA.

Sanishvili, R., Yakunin, A.F., Laskowski, R.A., Skarina, T., Evdokimova, E., Doherty-Kirby, A., Lajoie, G.A., Thornton, J.M., Arrowsmith, C.H., Savchenko, A., et al. 2003. Integrating structure, bioinformatics, and enzymology to discover function: BioH, a new carboxylesterase from *Escherichia coli*. *J. Biol. Chem.* **278:** 26039–26045.

Schneider, T.R. and Sheldrick, G.M. 2002. Substructure solution with SHELXD. *Acta Crystallogr. D Biol. Crystallogr.* **58:** 1772–1779.

Schultz, D.C., Vanderveer, L., Berman, D.B., Hamilton, T.C., Wong, A.J., and Godwin, A.K. 1996. Identification of two candidate tumor suppressor genes on chromosome 17p13.3. *Cancer Res.* **56:** 1997–2002.

Terwilliger, T.C. 2003. SOLVE and RESOLVE: Automated structure solution and density modification. *Methods Enzymol.* **374:** 22–37.

Thompson, J.D., Higgins, D.G., and Gibson, T.J. 1994. CLUSTAL W: Improving the sensitivity of progressive multiple sequence alignment through sequence weighting, position-specific gap penalties and weight matrix choice. *Nucleic Acids Res.* **22:** 4673–4680.

Vagin, A.A. and Isupov, M.N. 2001. Spherically averaged phased translation function and its application to the search for molecules and fragments in electron-density maps. *Acta Crystallogr. D Biol. Crystallogr.* **57:** 1451–1456.

van Pouderoyen, G., Eggert, T., Jaeger, K.E., and Dijkstra, B.W. 2001. The crystal structure of *Bacillus subtilis* lipase: A minimal α/β hydrolase fold enzyme. *J. Mol. Biol.* **309:** 215–226.

Wei, Y., Schottel, J.L., Derewenda, U., Swenson, L., Patkar, S., and Derewenda, Z.S. 1995. A novel variant of the catalytic triad in the *Streptomyces scabies* esterase. *Nat. Struct. Biol.* **2:** 218–223.

Yakunin, A.F., Yee, A.A., Savchenko, A., Edwards, A.M., and Arrowsmith, C.H. 2004. Structural proteomics: A tool for genome annotation. *Curr. Opin. Chem. Biol.* **8:** 42–48.

Zarembinski, T.I., Hung, L.W., Mueller-Dieckmann, H.J., Kim, K.K., Yokota, H., Kim, R., and Kim, S.H. 1998. Structure-based assignment of the biochemical function of a hypothetical protein: A test case of structural genomics. *Proc. Natl. Acad. Sci.* **95:** 15189–15193.

Zhou, C.Z., Meyer, P., Quevillon-Cheruel, S., De La Sierra-Gallay, I.L., Collinet, B., Graille, M., Blondeau, K., Francois, J.M., Leulliot, N., Sorel, I., et al. 2005. Crystal structure of the YML079w protein from *Saccharomyces cerevisiae* reveals a new sequence family of the jelly-roll fold. *Protein Sci.* **14:** 209–215.